Shot-noise-limited detection of absorbance changes induced by subpicojoule laser pulses in optical pump-probe experiments

Sergei Savikhin
Ames Laboratory-USDOE and Department of Chemistry, Iowa State University, Ames, Iowa 50011

(Received 27 April 1995; accepted for publication 26 May 1995)

We describe a high-frequency modulation and detection system capable of measuring absorbance changes ΔA on the order of 10^{-6} in optical pump-probe experiments using submilliwatt laser powers from a mode-locked ultrafast laser. For probe beam powers $\geqslant 9$ μW, the system offers nearly shot-noise-limited performance. © *1995 American Institute of Physics.*

I. INTRODUCTION

The optical pump-probe technique is a widely used method in ultrafast spectroscopy.[1] A pump pulse initiates optical changes in the sample, and a subsequent probe pulse monitors the changes at variable time delay. Current mode-locked Ti:sapphire lasers can provide ultrashort pulses with energies of up to 25 nJ at repetition rate ~100 MHz (~2.5 W of cw power); such pulses may cause absorbance changes ΔA on the order of 0.01 when sharply focused. In many systems of interest, such high powers may cause unwanted side effects, such as multiphoton absorption and annihilation. The latter effect is especially important in studying photosynthetic systems, which function physiologically only under very low light intensities $\leqslant 0.2$ W/cm^2. Specialized modulation schemes are necessary for detecting the small absorbance changes caused by such low light intensities. Since the noise in modern ultrafast mode-locked (ML) lasers (such as dye, Ti:sapphire or color center lasers) becomes nearly shot-noise-limited at frequencies >3 MHz,[2-4] successful modulation schemes place the signal content at a radio frequency (rf). In multiple modulation techniques, the pump and probe beams are modulated at different frequencies f_1 and f_2, and the signal is detected at sum- or difference-frequency $f_1 \pm f_2$. These techniques offer additional advantages in suppressing both scattered pump light and electrical modulation from the optical modulators.[5-9]

Bado *et al.*[5] used an amateur radio receiver tuned to a sum- or difference-frequency $f_1 \pm f_2$, a mechanical chopper provided audio-frequency (af) modulation of the pump beam. Subsequent amplitude modulation detection resulted in near shot-noise-limited (NSNL) performance at 36 mW beam intensity. Andor *et al.*[6] used a radio receiver in a single-sideband (SSB) scheme, where the signal-carrying sum frequency f_1+f_2 was mixed with a reference frequency $f_R=f_1+f_2$ to recover the af signal. The af signal was then detected by a lock-in amplifier (LIA), and NSNL performance was reported at 20 mW beam intensity. Anfinrud and Struve[7] excluded af modulation in their SSB detection scheme, which was also based on a radio receiver. Signal and reference frequencies were both downconverted to the af regime, and were then mixed in the LIA. This scheme provided NSNL performance at 10 mW laser power. Chwalek *et al.*[8] used similar downconversion with a single-beam modulation scheme, but designed a custom mixer system in place of a radio receiver. While a specialized rf LIA could be used in the detection scheme,[9] their noise level and dynamic range are typically less favorable than that of conventional af LIAs.[8] Downconversion offers a unique combination of rf modulation in the region of minimal laser noise, with the excellent performance of af LIAs.

The apparatus presented here is a modification of one described previously.[7] Both the modulation and detection parts of the system have been modified, resulting in near shot-noise-limited performance at laser powers as low as 9 μW. It offers simpler design, as well as versatility between single and multiple beam modulation. For illustration, absorbance changes on the order of 10^{-6} were detected in a test sample (HITCI dye solution) at laser powers as low as ≈ 50 μW. This corresponds to a single laser pulse energy of <1 pW.

II. MODULATION

A single modulation scheme may be realized using two base oscillators, producing frequencies $f_1=6.5$ MHz and $f_R=7$ MHz. The reference frequency 7 MHz was chosen after Anfinrud and Struve,[7] corresponding to an rf regime where many ultrafast lasers provide NSNL performance. A possible block diagram is shown in Fig. 1(a). Each frequency is split using power splitters. After passing the 20 dB attenuators and the amplifiers, the 7.0 and 6.5 MHz frequencies are mixed in double-balanced mixers. The resulting $f_2=0.5$ MHz output is then filtered with a BLP-1.9 low pass filter, amplified, and filtered by another 0.5 MHz low pass filter to provide better isolation from the other frequencies. The amplifiers and attenuators prior to the mixer enhance mutual isolation between the 6.5 and 7 MHz frequencies. The choice of the more involved scheme described in the following was dictated only by the availability of oscillators in our laboratory.

The modulation block diagram actually used in our prototype experiments is shown in Fig. 1(b). The base high frequencies were derived from three separate oscillators operating at frequencies f_A, f_B, and f_C ($f_A > f_B > f_C$) with output levels 1–2 V (13–19 dBm). f_A was generated in a PTS-160 (Programmed Test Sources, Inc.) frequency synthesizer, while f_B and f_C were provided by crystal oscillators in two Harris Corp. mode locker drivers. Each of the three frequencies was split using power splitters and passed through high pass filters. The two modulation frequencies f_1 and f_2 and

 0034-6748/95/66(9)/4470/5/$6.00

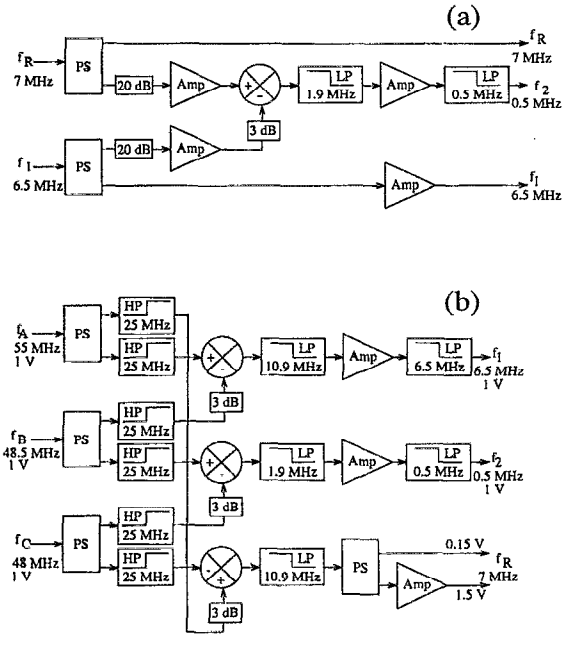

FIG. 1. Block diagram of frequency syntheses: (a) based on two oscillators; (b) used in the present work. Amplifiers (Amp) [Comlinear E103-I-BNC-50-50-20]; Power splitters (PS) [Mini-Circuits ZSC-2-1]; High-Pass (HP) filters [Mini-Circuits BHP-25]; low-pass (LP) filters: 1.9 MHz (Mini-Circuits BLP-1.9), 10.9 MHz (Mini-Circuits BLP-10.9), 6.5 MHz (Chesterfield Products P/N 22-10-2045), 0.5 MHz (5-pole Cauer–Chebyshev filter); attenuators: 20 dB (Mini-Circuits CAT-20), 3 dB (Mini-Circuits CAT-3); mixers (Mini-Circuits ZAD-3SH).

the reference sum frequency f_R were synthesized from the three possible combinations of f_A, f_B, and f_C in double-balanced mixers:

$$f_1=f_A-f_B, \quad f_2=f_B-f_C, \quad f_R=f_A-f_C. \tag{1}$$

The mixer outputs were filtered using low-pass filters. The two modulation frequencies f_1 and f_2 were then amplified 10 times in amplifiers, and were low-pass filtered again to provide maximum isolation between frequencies. The reference signal f_R was split into two. The 0.15 V output was used for the reference frequency in the detection system; the amplified 1.5 V output was used to modulate the pump beam when the single-modulation scheme was chosen. Six high-pass filters improved the isolation between channels by blocking the output frequencies from entering the neighboring channels via backpropagation through the splitters. Additional 3 dB fixed attenuators at the LO inputs of the mixers provided optimal mixing signal levels. All components were inexpensive miniature front-end units with standard BNC-connectors. This facilitated assembly of the modulation apparatus; cables were avoided by connecting components directly together with BNC adapters.

Changes in the frequencies f_A, f_B, and/or f_C cause shifts in the output frequencies f_1, f_2, and f_R, in such a way that the sum-frequency modulation condition $f_R=f_1+f_2$ is automatically maintained according to Eq. (1). In the present system, we used the frequencies $f_A=55$ MHz, $f_B=48.5$ MHz, and $f_C=48$ MHz; this resulted in $f_1=6.5$ MHz, $f_2=0.5$ MHz, and $f_R=7$ MHz.

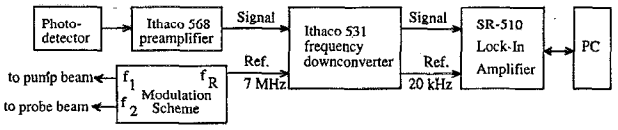

FIG. 2. Block diagram of the pump-probe detection system.

The isolation of f_2 channel from f_R is most critical for double beam modulation, where f_2 modulates the probe beam. The described circuit provided $\geqslant$180 dB isolation of f_2 from f_R. The isolation of f_1 from f_R is not so critical, and was 60 dB in our case.

In the double-beam modulation technique, the frequencies f_1 and f_2 were passed through variable attenuators (Merrimac ARC-4, not shown), and directed to acousto-optic modulators AOM (Intra-Action 80NR) to modulate the pump and probe beams, respectively. Both beams were derived from a single Ti:sapphire self mode-locked fs laser output using a beam splitter. They were passed through AOMs, and crossed in the sample using 20 cm focal length lens. The spot size in the sample was 110 μm full width at half maximum (FWHM). The negative group velocity dispersion (GVD) in 1.9 cm of SF-4 glass used in AOM can significantly broaden the initially short laser pulses. Therefore, a pair of SF-10 glass Brewster angle prisms separated by 45 cm were used in a standard double-pass scheme prior to a pump-probe apparatus to introduce positive GVD, and thus precompensate for the broadening. This precompensation worked well for pulses as short as 40 fs (at ~800 nm). For shorter pulses, a thinner AOM should be used (1 cm thick Intra-Action AOM-85.6NR, for example); use of the same optical materials in AOM's and precompensating prisms is recommended. In more detail, the one- and two-color pump-probe optics have been described previously.[10] In the alternative single-modulation scheme, the pump beam alone was modulated at frequency f_R.

III. DETECTION

An Ithaco Dynatrac 531 high-frequency downconverter shifted the signal at the rf frequency f_R to the fixed frequency 20 kHz (Fig. 2). The advantages of using a downconverter instead of a radio receiver[6,7] include simplicity, improved linearity, and higher dynamic range. An Ithaco 568 low-noise preamplifier amplified the rf signal prior to downconversion. The downconverter output was processed by a standard af LIA (Stanford Research Systems SR-510). The downconverter gain was $\times 1$ and the input impedance was 50 Ω; the preamplifier gain was 40 dB. The preamplifier was packed into a copper wire net directly grounded to the laser tabletop for extra shielding; this proved to be crucial for eliminating background due to rf pickup in the preamplifier.

The modulated probe beam was detected by a Hamamatsu S1721 fast photodiode; similar results were obtained with an EG&G FOD-100 photodiode. Both photodiodes have a relatively large active area (5.1 mm ^{2}), simplifying optical alignment. While it is widely believed that

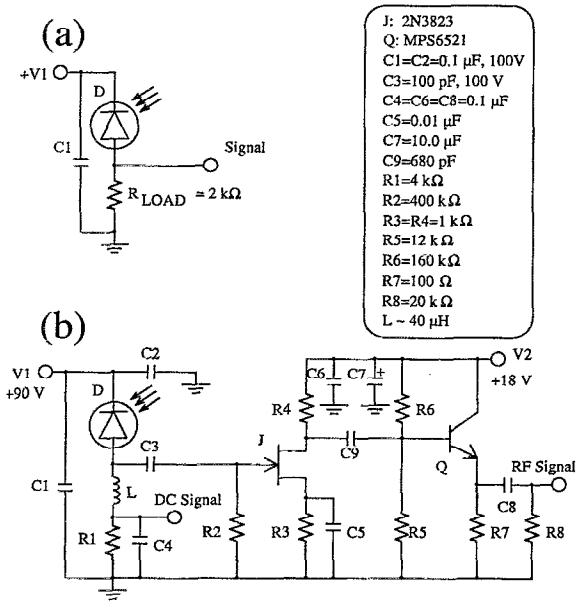

FIG. 3. Detailed schematic of photodetector head: (a) low-sensitivity version, NEP~100 pW/$\sqrt{\text{Hz}}$ (with Ithaco 568 preamplifier); (b) high-sensitivity resonant detector, NEP=1.9 pW/$\sqrt{\text{Hz}}$.

photomultipliers provide better sensitivity, their typical maximal illumination levels are in picowatt region, where the shot-noise level is in the order of 10^{-4} (for 1 s accumulation time). In contrast, for light powers in the μW region and higher, silicon photodiodes provide noise levels $<10^{-6}$ (NSNL performance) with $\geq$40% quantum efficiency in the wide spectral region 300–1050 nm ($\geq$80% for 550–950 nm).

In the simplest scheme, the photodiode was connected directly to a load resistor [Fig. 3(a)]. While the specified preamplifier input impedance is 1 G Ω, its input capacitance (together with the capacitance of connectors, cables, and photodiode junction) yields far lower rf impedances (several hundred Ω) and thus drastically reduces sensitivity. The noise equivalent power (NEP) for this scheme was ~100 pW/$\sqrt{\text{Hz}}$ at 754 nm laser wavelength; it was limited only by intrinsic preamplifier noise. (The NEP is thereafter defined as the root mean square of the optical power required to produce signal equivalent to noise in a 1 Hz bandwidth at 7 MHz.) Another drawback of this scheme is its flat frequency response. While the 0.5 MHz p-p modulation in the probe beam is comparable to the laser intensity, it is typically 5–6 orders of magnitude larger than the 7 MHz signal. Preliminary signal filtering is thus desirable in order to avoid preamplifier saturation.

This function is realized in the photodetector head [Fig. 2(b)], which acts as a 7 MHz light antenna and narrowband signal amplifier. Since the junction capacitance C_D is intrinsic to the photodiode, the parallel resonant LC circuit (which was precisely tuned to 7 MHz) incorporates C_D along with the other parasitic capacitances. The low-noise N-channel JFET transistor J, operating in the common-source mode, isolated the LC circuit from the subsequent amplification stage. The resonant circuit comprised the inductor L in parallel with C_D, the JFET capacitance C_J, and the parasitic capacitances of wires and resistors. $C3$ provided rf coupling between C_D and C_J, $C2$, and $C4$ provided an rf ground to the upper pin of C_D and the lower pin of inductor L. In this configuration, the 7 MHz photodiode signal was picked up and resonantly amplified by the LC circuit. This yielded 1000-fold suppression of the 0.5 MHz component relative to the 7 MHz component. $R1$ and $C4$ provided a dc output proportional to the average probe beam power. A photodiode-based dc power meter was placed into the pump beam path for routine normalization of profiles to the pump and probe intensities.[10]

The second amplification stage incorporated a low-noise npn transistor Q and served as an output impedance transformer (current amplifier). Capacitor $C8$ added additional losses for low frequencies. The dc voltage on the emitter of Q, determined by $R5/R6$ voltage divider, was set to ~0.5 V to minimize power consumption. Transistors J and Q together consumed about 10 mA, and were powered by an 18 V battery pack to eliminate possible power supply pickup. A 90 V battery supplied the photodiode bias.

The photodetector was built inside a 85×45×30 mm^3 shielded box of double-sided copper clad. Four BNC connectors provided feedthroughs for the dc and rf signals and for the +18 and +90 V supply voltages. The top cover was secured with screws; several flat springs around the box perimeter improved shielding.

The resonance frequency was tuned by adjusting the number of turns in inductor L, wound on a high-frequency ferrite toroid (≈10 mm diam). The inductance is typically ~40 μH. During tuning, the probe beam was modulated at 7 MHz and its power was reduced to a few nW. The output of the detector head at 7 MHz was monitored through an Ithaco 568 preamplifier on a standard oscilloscope. The exact position for maximum amplification was found by changing probe beam modulation frequency; the number of turns in L was increased for frequencies higher than 7 MHz, and reduced for lower frequencies.

IV. RESULTS AND DISCUSSION

The front-end sensitivity of the detection system was calibrated using a 754 nm probe beam modulated at f_R=7 MHz. The 1 nW peak-to-peak modulation of the probe beam produced a 1 mV reading in the LIA. The system responsivity was thus 10^6 V/W. To ensure maximal precision, the peak-to-peak modulation amplitude at 7 MHz was determined independently by Fourier analysis of the probe beam waveform, which was measured by a fast photodiode with flat frequency response.

The dark NEP of the detection system at 754 nm was determined to be 2.4 pW/$\sqrt{\text{Hz}}$; the preamplifier with grounded input contributed 0.62 pW/$\sqrt{\text{Hz}}$. The NEP of the photodetector head was therefore $\sqrt{2.4^2-0.62^2}\approx$2.3 pW/$\sqrt{\text{Hz}}$. At 900 nm (the wavelength of maximal diode responsivity), the NEP was estimated to be 1.9 pW/$\sqrt{\text{Hz}}$. For comparison, the New Focus Model 1811 amplified rf photodetector has comparable NEP (2.5 pW/$\sqrt{\text{Hz}}$); however, its small

active area 0.07 mm^2 as well as its flat frequency response from DC to 125 MHz are less advantageous for our application.

The shot-noise current I_{rms} in the photodiode is related to the dc current I_{dc} by

$$I_{rms}=\sqrt{2eI_{dc}B}, \tag{2}$$

where e is the electron charge and B is the frequency bandwidth. This can be rewritten in terms of the optical power P and the noise equivalent power P_{rms} as

$$P_{rms}=\sqrt{\frac{2ePB}{r}}, \tag{3}$$

where r is photodiode responsivity. At 754 nm, r=0.5 A/W, and near shot-noise-limited performance is predicted with optical powers down to $P = (rP_{rms}^2)/(2eB) = 9$ μW. This is three orders of magnitude lower than that reported in Ref. 7. We have measured the noise levels corresponding to the probe beam powers 6 μW and 110 μW. The measured NEP values were 4.0 pW/$\sqrt{\text{Hz}}$ and 13 pW/$\sqrt{\text{Hz}}$, respectively, which are in reasonable accordance with the calculated shot-noise levels 2 pW/$\sqrt{\text{Hz}}$ and 8.4 pW/$\sqrt{\text{Hz}}$.

The 0.5 MHz probe beam modulation component (which is still present in the photodetector output) is generally filtered out by the downconverter. However, this component saturates the preamplifier at beam powers >0.5 mW, causing a decrease in system responsivity. The critical power level can be raised to 5 mW by simply switching the preamplifier into 20 dB mode; in this case, the dark NEP was 4 pW/$\sqrt{\text{Hz}}$, considerably lower than the shot-noise-limit. For probe powers >5 mW, a 7 MHz bandpass filter may be added between the photodetector head and preamplifier. In practice, the shot-noise level in ΔA profiles measured with a ~1 mW probe beam is on the order of 10^{-8}, which is more than enough for most applications.

To illustrate the possibilities of the system, it was applied to measurements of pump-probe profiles of a test dye solution HITCI in methanol. A Ti:sapphire laser provided nearly transform limited ~70 fs long pulses, centered at 754 nm with a 76 MHz repetition rate. The sample was housed in a centrifugal cell;[10] the optical density at 754 nm was 0.3 in the 0.7 mm cell path length. The laser power was divided approximately evenly between pump and probe beams. The LIA time constant was 1 s, which corresponds to equivalent bandwidth 0.25 Hz (6 dB roll-off RC-filter). The absorbance changes ΔA induced by the modulated pump beam were calculated according to the formula

$$\Delta A=\frac{S_{rf}}{S_{DC}\ln(10)}, \tag{4}$$

where S_{rf} and S_{dc} are the peak-to-peak probe beam modulation at 7 MHz and the probe beam dc power, respectively. Both quantities were measured after the probe beam passed the sample. The noise in measured time-resolved profiles was calculated as a root mean square χ, and compared to the signal level S_{rf} at 1 ps delay. Figure 4 shows pump-probe profiles recorded with several laser powers in the double- and single-beam modulation schemes; some of the data characteristics are listed in Table I.

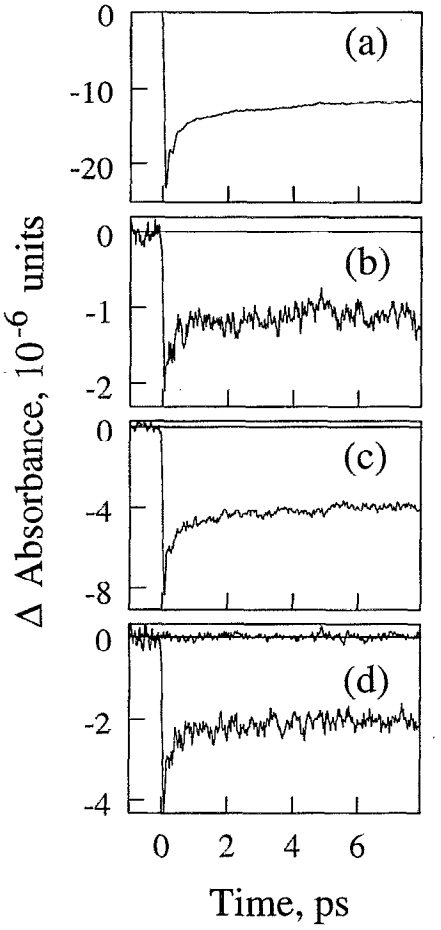

FIG. 4. Pump-probe profiles measured in HITCI with LIA time constant 1 s: (a) double beam modulation, laser power 760 μW; (b) double beam modulation, 72 μW; (c) single beam modulation, 72 μW; (d) single beam modulation, 44 μW, superimposed on dark noise profile. ΔA values are given in absolute units.

Pump intensities as low as 22 μW still provided reasonable signal-to-noise ratios, which could be improved by signal averaging. The corresponding single pulse energy is only 0.3 pJ or 10^6 photons per pulse; the integrated power density (0.22 W/cm^2) is comparable to the intensity of sunlight, although the latter is spread over a wider spectrum.

When using double modulation, one should bear in mind

TABLE I. Pump-probe signal and signal-to-noise values measured at various laser intensities in single- and double-modulation schemes. Pump and probe beam modulation depths were ~70%.

Modulation type	Pump+probe power, μW	ΔA at 1 ps	Signal-to-noise S/χ
Double	760	1.4×10^{-5}	180
Double	210	2.8×10^{-6}	45
Double	72	1.2×10^{-6}	10
Single	72	4.8×10^{-6}	30
Single	44	2.3×10^{-6}	14

that the absorbance modulation actually provided by a pump beam is about four times larger than the ΔA signal measured at the sum frequency (Table I). The advantage of double beam modulation lies in suppression of background signal arising from the scattered pump beam. Even with such a high optical quality sample as a dye solution, the background level was several times higher than the signal itself.

The detection wavelength is not limited to the one used in this example. We used this system to study ultrafast processes in various samples at wavelengths from 684 nm (our "bluest" Ti:sapphire output wavelength) to 850 nm. Taking into account the wide Ti:sapphire spectral tuning range, along with the availability of second, third, and fourth harmonics and optical parametric oscillators, experiments at virtually any wavelength from ~200 nm to ~1.1 μm can be performed (this range is limited by the photodiode). The high sensitivity of the system facilitates experiments at the extreme edges of tuning ranges. Another attractive two-color pump-probe technique, where two different spectral shapes are extracted from the same broadband Ti:sapphire output by interference filters,[10] can be effectively used in combination with this high-sensitivity detection system. The system described here is not restricted to the Ti:sapphire laser, it can be used with any source of short light pulses operating at repetition rates $\geq$40 MHz.

In conclusion, we have designed a high-frequency pump-probe modulation and detection scheme capable of using with pump-probe pulse energies in the pJ region and power densities ~1 W/cm^2. The system may be used with any ML (or CW) laser with repetition rate $\geq$40 MHz. Absorbance changes on the order of 10^{-6} are easily detected for a test HITCI dye sample. The system offers near shot-noise-limited performance at probe powers >9 μW, and has been successfully used in ultrafast studies of photosynthetic biological and artificial systems.

ACKNOWLEDGMENTS

The Ames Laboratory is operated for the U. S. Department of Energy by Iowa State University under Contract No. W-7405-Eng-82. This work was supported by the Division of Chemical Sciences, Office of Basic Energy Sciences. The author is indebted to Walter S. Struve for his assistance and useful discussions.

[1] G. R. Fleming, *Chemical Applications of Ultrafast Spectroscopy*, The International Series of Monographs on Chemistry (Oxford University Press, Clarendon Press, 1986).
[2] T. M. Baer and D. D. Smith, *Ultrafast Phenomena IV*, edited by D. H. Auston and K. B. Eisenthal (Springer, Berlin, 1984), p. 96.
[3] J. Son, J. V. Rudd, and J. F. Whitaker, Opt. Lett. **17**, 733 (1992).
[4] U. Keller, C. E. Soccolich, G. Sucha, M. N. Islam, and M. Wegener, Opt. Lett. **15**, 974 (1990).
[5] P. Bado, S. B. Wilson, and K. K. Wilson, Rev. Sci. Instrum. **53**, 706 (1982).
[6] L. Andor, A. Lörincz, J. Siemion, D. D. Smith, and S. A. Rice, Rev. Sci. Instrum. **55**, 64 (1984).
[7] P. Anfinrud and W. S. Struve, Rev. Sci. Instrum. **57**, 380 (1985).
[8] J. M. Chwalek and D. R. Dykaar, Rev. Sci. Instrum. **61**, 1273 (1990).
[9] E. L. Quitevis, E. F. Gudgin Templeton, and G. A. Kenney-Wallace, Appl. Opt. **24**, 318 (1985).
[10] S. Savikhin and W. S. Struve, Biochemistry **33**, 11200 (1994).